ISSN 1674-1056
http://cpb.iphy.ac.cn
http://iopscience.iop.org/cpb
中国物理 B
Chinese Physics
中国物理
Chinese Physics B

Steady-state entanglement and heat current of two coupled qubits in two baths without rotating wave approximation

Mei-Jiao Wang(王美姣), Yun-Jie Xia(夏云杰)

Citation: Chin. Phys. B . 2019, 28(6): 060303. **doi:** 10.1088/1674-1056/28/6/060303
Journal homepage: http://cpb.iphy.ac.cn; http://iopscience.iop.org/cpb

What follows is a list of articles you may be interested in

Phase effect on dynamics of quantum discord modulated by interaction between qubits

Wang Guo-You, Guo You-Neng, Zeng Hao-Sheng
Chin. Phys. B . 2015, 24(9): 090303. **doi:** 10.1088/1674-1056/24/9/090303

Hybrid double-dot qubit measurement with a quantum point contact

Yan Lei, Yin Wen, Wang Fang-Wei
Chin. Phys. B . 2014, 23(10): 100303. **doi:** 10.1088/1674-1056/23/10/100303

Entanglement and non-Markovianity of a spin-*S* system in a dephasing environment

Fan Zi-Long, Tian Jing, Zeng Hao-Sheng
Chin. Phys. B . 2014, 23(6): 060303. **doi:** 10.1088/1674-1056/23/6/060303

Engineering steady-state entanglement for two atoms held in separate cavities through laser cooling

Shen Li-Tuo, Chen Rong-Xin, Wu Huai-Zhi, Yang Zhen-Biao
Chin. Phys. B . 2014, 23(4): 040303. **doi:** 10.1088/1674-1056/23/4/040303

Comparison between non-Markovian dynamics with and without rotating wave approximation

Tang Ning, Xu Tian-Tian, Zeng Hao-Sheng
Chin. Phys. B . 2013, 22(3): 030304. **doi:** 10.1088/1674-1056/22/3/030304

Steady-state entanglement and heat current of two coupled qubits in two baths without rotating wave approximation*

Mei-Jiao Wang(王美姣)[1,2] and Yun-Jie Xia(夏云杰)[1,2,†]

[1] College of Physics and Engineering, Qufu Normal University, Qufu 273165, China
[2] Shandong Provincial Key Laboratory of Laser Polarization and Information Technology, Qufu Normal University, Qufu 273165, China

(Received 21 January 2019; revised manuscript received 11 March 2019; published online 8 May 2019)

We study the steady-state entanglement and heat current of two coupled qubits, in which two qubits are connected with two independent heat baths (IHBs) or two common heat baths (CHBs). We construct the master equation in the eigenstate representation of two coupled qubits to describe the dynamics of the total system and derive the solutions in the steady-state with stronger coupling regime between two qubits than qubit–baths. We do not make the rotating wave approximation (RWA) for the qubit–qubit interaction, and so we are able to investigate the behaviors of the system in both the strong coupling regime and the weak coupling regime, respectively. In an equilibrium bath, we find that the entanglement decreases with the bath temperature and energy detuning increasing under the strong coupling regime. In the weak coupling regime, the entanglement increases with coupling strength increasing and decreases with the bath temperature and energy detuning increasing. In a nonequilibrium bath, the entanglement without RWA is useful for entanglement at lower temperatures. We also study the heat currents of the two coupled qubits and their variations with the energy detuning, coupling strength and low temperature. In the strong (weak) coupling regime, the heat current increases (decreases) with coupling strength increasing when the temperature of one bath is lower (higher) than the other, and the energy detuning leads to a positive (negative) effect when the temperature is low (high). In the weak coupling regime, the variation trend of heat current is opposite to that of coupling strength for the IHB case and the CHB case.

Keywords: steady-state entanglement, equilibrium and nonequilibrium baths, heat current, rotating wave approximation

PACS: 03.65.Yz, 05.30.–d, 05.70.Ln **DOI:** 10.1088/1674-1056/28/6/060303

1. Introduction

Quantum entanglement[1,2] plays a central role in quantum information processing (QIP)[3] and has attracted considerable attention. In a practical application, quantum systems are never completely isolated from the environment and the quantum behavior may be substantially affected by unwanted couplings to their surroundings. The prepared entanglement may vanish because of the decoherence effect[4] of environments. A more practical situation for the open quantum system is in a nonequilibrium thermal bath with a nonvanishing temperature difference. Applying the temperature gradient has enabled many quantum thermal devices to be proposed, such as thermal rectifiers,[5–9] thermal diodes,[10,11] thermal transistors,[12] self-contained refrigerators,[13–18] and the quantum Otto cycle.[19–21]

We study the quantum entanglement of a system in the steady-state, in contrast to the generation of transient entanglement. When the coupled systems contact the thermal baths and reach thermal equilibrium, the steady-state entanglement may arise in the long-time limit. Mathematically, the thermalization time for a system should be infinite because the long-time limit (limit $t \to \infty$) is needed to make sure that these density matrix elements evolve to their steady-state values. From the viewpoint of physics, we might introduce some time scales to describe thermalization as the half-life of an exponential decay. However, for the present systems, the evolutions of these density matrix elements are not purely exponential functions. At the same time, these evolutions also depend on the initial conditions.

To solve the steady-state entanglement of the system, we use an example of a practical approach that is based on the master equations for the reduced density operator,[22,23] which is extensively employed to describe the dynamics of quantum systems weakly coupled to reservoirs. The quantum system of interest may be constituted by one or multiple subsystems and connected with many environments.[24–31] However, in this literature, both the interactions between subsystems and the system and the baths are subject to the RWA. In Ref. [32], there is no RWA between two qubits, but one of them is independent, and only one of them interacts with a bath. However, the individual subsystems of the coupled systems are difficult to isolate from contacting their own local baths.

Focusing on this situation, in this paper we study the steady-state entanglement and heat current of two coupled qubits, in which two qubits are connected with two independent heat baths (IHBs) or two common heat baths (CHBs),

*Project supported by the National Natural Science Foundation of China (Grant Nos. 61675115 and 11704221).
†Corresponding author. E-mail: yjxia@qfnu.edu.cn
© 2019 Chinese Physical Society and IOP Publishing Ltd

and the coupling strength between two subsystems is stronger than the system–bath coupling. When the coupling strength is stronger than the system–bath coupling, the composite quantum system can be regarded as a single system. The evolution process to the steady-state can be modeled by a quantum master equation. We do not make RWA for the qubit–qubit interaction, therefore we are able to investigate the behavior of the system in both the strong coupling regime and weak coupling regime. Calculations are performed for a wide range of values of qubit–qubit coupling strengths as well as energy detuning of the subsystems and the temperature gradient of the baths. As another figure of merit, we also consider the heat current with respect to a bath of two qubits, observing how the heat current varies with the energy detuning, coupling strength and diverse lower temperatures.

The remainder of this paper is organized as follows. In Section 2, we present the physical model and the derivation of the master equation. In Section 3, we give the steady-state entanglement of the IHB case and CHB case. In Section 4, we consider the heat current of the IHB case and CHB case. We draw some conclusions from the present study in Section 5.

2. Physical model and the derivation of the master equation

As described in the schematic diagram in Fig. 1, we consider a total model consisting of two coupled qubits A, B and a non-equilibrium environment of two heat baths which are bath a: having temperature T_1 and bath b: having temperature T_2. With system–environment interaction, the total Hamiltonian of the system and two baths can be divided into three parts as follows:

$$H = H_{\rm S} + H_{\rm B} + H_{\rm I}. \tag{1}$$

Here, $H_{\rm S}$ is the Hamiltonian of two coupled qubits, $H_{\rm B}$ is the Hamiltonian of two heat baths, $H_{\rm I}$ is the interaction Hamiltonian between two qubits and two heat baths.

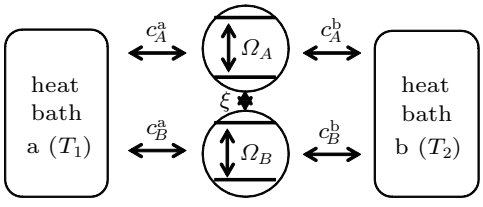


Fig. 1. Schematic diagram of physical model with two coupled qubits A and B interacting with a non-equilibrium environment consisting of bath a and bath b. Coupling coefficients c_i^R, $i = A, B$, $R =$ a, b, determine configuration of interaction channels.

The Hamiltonian $H_{\rm S}$ reads as (we take $\hbar = 1$)

$$\begin{aligned} H_{\rm S} =\ & \Omega_A \sigma_A^+ \sigma_A^- + \Omega_B \sigma_B^+ \sigma_B^- \\ & + \xi \left(\sigma_A^+ \sigma_B^- + \sigma_A^- \sigma_B^+ + \sigma_A^+ \sigma_B^+ + \sigma_A^- \sigma_B^- \right), \end{aligned} \tag{2}$$

where $\sigma_{A(B)}^+ = |1\rangle_{A(B)} \langle 0|$ ($\sigma_{A(B)}^- = |0\rangle_{A(B)} \langle 1|$) is the raising (lowering) operator for two qubits A and B; Ω_A and Ω_B are the bare frequencies of two qubits, and coupled with each other by the dipole–dipole interaction of strength ξ.

The Hilbert space of two coupled qubits may be spanned by the following four bare states: $\eta_1 = |11\rangle$, $\eta_2 = |10\rangle$, $\eta_3 = |01\rangle$, and $\eta_4 = |00\rangle$, which are eigenstates of the free Hamiltonian $\Omega_A \sigma_A^+ \sigma_A^- + \Omega_B \sigma_B^+ \sigma_B^-$, with the corresponding eigenenergies $E_{\eta_1} = \Omega_m$, $E_{\eta_2} = \Omega_A$, $E_{\eta_3} = \Omega_B$, and $E_{\eta_4} = 0$. Here, we have introduced the total energy $\Omega_m = \Omega_A + \Omega_B$ and the energy detuning $\Delta\Omega = \Omega_A - \Omega_B$.

Due to the dipole–dipole interaction and the strong coupling regime between the subsystems, we construct a master equation to describe the evolution of the system in the eigenstate representation. We can solve the eigenequation $H_{\rm S} |\lambda_p\rangle = E_p |\lambda_p\rangle$ ($p = 1, 2, 3, 4$) to obtain the following four eigenstates and eigenvalues:

$$\begin{aligned} & |\lambda_1\rangle = \alpha_+ |\eta_1\rangle + \alpha_- |\eta_4\rangle, \quad |\lambda_2\rangle = \beta_+ |\eta_2\rangle + \beta_- |\eta_3\rangle, \\ & |\lambda_3\rangle = -\beta_- |\eta_2\rangle + \beta_+ |\eta_3\rangle, \quad |\lambda_4\rangle = -\alpha_- |\eta_1\rangle + \alpha_+ |\eta_4\rangle, \\ & E_1 = \frac{1}{2}\left(\Omega_m + \sqrt{\Omega_m^2 + 4\xi^2} \right), \\ & E_2 = \frac{1}{2}\left(\Omega_m + \sqrt{\Delta\Omega^2 + 4\xi^2} \right), \\ & E_3 = \frac{1}{2}\left(\Omega_m - \sqrt{\Delta\Omega^2 + 4\xi^2} \right), \\ & E_4 = \frac{1}{2}\left(\Omega_m - \sqrt{\Omega_m^2 + 4\xi^2} \right), \end{aligned} \tag{3}$$

where

$$\alpha_\pm = \frac{1}{\sqrt{2}} \sqrt{1 \pm \frac{\Omega_m}{\sqrt{\Omega_m^2 + 4\xi^2}}}$$

and

$$\beta_\pm = \frac{1}{\sqrt{2}} \sqrt{1 \pm \frac{\Delta\Omega}{\sqrt{\Delta\Omega^2 + 4\xi^2}}}.$$

Hence, the eigenstructure for the system Hamiltonian is given by

$$H_{\rm S} = \sum_{p=1}^{4} E_p \left|\lambda_p\right\rangle \langle \lambda_p|. \tag{4}$$

In this paper, we consider the two harmonic-oscillator heat baths. The Hamiltonian $H_{\rm B}$ of two baths reads as

$$H_{\rm B} = \sum_j \omega_{aj} a_j^\dagger a_j + \sum_k \omega_{bk} b_k^\dagger b_k, \tag{5}$$

where $a_j^\dagger$ ($b_k^\dagger$) and a_j (b_k) are the creation and annihilation operators of the j-th (k-th) harmonic oscillator with frequency ω_{aj} (ω_{bk}), respectively. The interaction Hamiltonian $H_{\rm I}$ between two qubits and two baths is

$$\begin{aligned} H_{\rm I} =\ & c_A^{\rm a} \sigma_A^x \otimes \sum_j g_{Aj} \left(a_j + a_j^\dagger \right) \\ & + c_B^{\rm a} \sigma_B^x \otimes \sum_j g_{Bj} \left(a_j + a_j^\dagger \right) \end{aligned}$$

$$+c_A^{\rm b}\sigma_A^x\otimes\sum_k g_{Ak}\left(b_k+b_k^\dagger\right)$$
$$+c_B^{\rm b}\sigma_B^x\otimes\sum_k g_{Bk}\left(b_k+b_k^\dagger\right), \tag{6}$$

where $\sigma_i^x=\sigma_i^+ +\sigma_i^-$ $(i=A,B)$, g_{Aj}, g_{Bj}, g_{Ak}, g_{Bk} are the interaction strengths between qubit–bath. For simplicity, we assume that they are real numbers.

According to the distribution of the coupling strengths between the i-th atom and the R-th bath, our model can be analyzed via the following two cases, *i.e.*, IHB case and CHB case. For the IHB case, $c_A^{\rm a}=c_B^{\rm b}=1$ and $c_A^{\rm b}=c_B^{\rm a}=0$, in which each atom interacts with an individual heat bath. For CHB case, $c_A^{\rm a}=c_B^{\rm b}=c_A^{\rm b}=c_B^{\rm a}=1$, in which the two atoms are coupled with both heat baths simultaneously. Without loss of generality, we derive the solutions in the CHB case. When we set $c_A^{\rm b}=c_B^{\rm a}=0$, the derivation degenerates to the IHB case.

In the presence of the weak coupling between qubits and baths, the equation of motion of the qubits can be derived within the framework of the Born–Markov approximation as

$$\dot\rho=-{\rm i}\left[H_{\rm S},\rho\right]+\sum_{R=a,b}\left(\zeta_A^R[\rho]+\zeta_B^R[\rho]+\zeta_{AB}^R[\rho]\right). \tag{7}$$

The Lindblad operator $\zeta_i^R[\rho]$ represents the dissipation of qubit $A(B)$ due to the heat bath-R and takes the form as

$$\begin{aligned}\zeta_i^R[\rho]=&\sum_{n=1,2}\gamma_i^R(\omega_n)\left[\bar n^R(\omega_n)+1\right]\left[2\sigma_i^x(\omega_n)\rho\sigma_i^{x+}(\omega_n)-\left\{\sigma_i^{x+}(\omega_n)\sigma_i^x(\omega_n),\rho\right\}\right]\\&+\sum_{n=1,2}\gamma_i^R(\omega_n)\bar n^R(\omega_n)\left[2\sigma_i^{x+}(\omega_n)\rho\sigma_i^x(\omega_n)-\left\{\sigma_i^x(\omega_n)\sigma_i^{x+}(\omega_n),\rho\right\}\right].\end{aligned} \tag{8}$$

While $\zeta_{AB}^R[\rho]$ reflects the collective behavior of two qubits as a single entity to emit or absorb photons induced by the common bath R in the form of

$$\begin{aligned}\zeta_{AB}^R[\rho]=&\sum_{n=1,2}\gamma_{AB}^R(\omega_n)\left[\bar n^R(\omega_n)+1\right]\left[2\sigma_A^x(\omega_n)\rho\sigma_B^{x+}(\omega_n)-\left\{\sigma_B^{x+}(\omega_n)\sigma_A^x(\omega_n),\rho\right\}\right]\\&+\sum_{n=1,2}\gamma_{AB}^R(\omega_n)\bar n^R(\omega_n)\left[2\sigma_A^{x+}(\omega_n)\rho\sigma_B^x(\omega_n)-\left\{\sigma_B^x(\omega_n)\sigma_A^{x+}(\omega_n),\rho\right\}\right]\\&+\sum_{n=1,2}\gamma_{AB}^R(\omega_n)\left[\bar n^R(\omega_n)+1\right]\left[2\sigma_B^x(\omega_n)\rho\sigma_A^{x+}(\omega_n)-\left\{\sigma_A^{x+}(\omega_n)\sigma_B^x(\omega_n),\rho\right\}\right]\\&+\sum_{n=1,2}\gamma_{AB}^R(\omega_n)\bar n^R(\omega_n)\left[2\sigma_B^{x+}(\omega_n)\rho\sigma_A^x(\omega_n)-\left\{\sigma_A^x(\omega_n)\sigma_B^{x+}(\omega_n),\rho\right\}\right],\end{aligned} \tag{9}$$

where

$$\sigma_i^x(\omega_1)=\langle\lambda_4|\sigma_i^x|\lambda_3\rangle|\lambda_4\rangle\langle\lambda_3|+\langle\lambda_2|\sigma_i^x|\lambda_1\rangle|\lambda_2\rangle\langle\lambda_1|$$

and

$$\omega_1=E_1-E_2=E_3-E_4=(\sqrt{\Omega_m^2+4\xi^2}-\sqrt{\Delta\Omega^2+4\xi^2})/2$$

corresponding to the transitions $|\lambda_1\rangle\leftrightarrow|\lambda_2\rangle$ and $|\lambda_3\rangle\leftrightarrow|\lambda_4\rangle$, while

$$\sigma_i^x(\omega_2)=\langle\lambda_3|\sigma_i^x|\lambda_1\rangle|\lambda_3\rangle\langle\lambda_1|+\langle\lambda_4|\sigma_i^x|\lambda_2\rangle|\lambda_4\rangle\langle\lambda_2|$$

and

$$\omega_2=E_1-E_3=E_2-E_4=(\sqrt{\Omega_m^2+4\xi^2}+\sqrt{\Delta\Omega^2+4\xi^2})/2$$

corresponding to the transitions $|\lambda_1\rangle\leftrightarrow|\lambda_3\rangle$ and $|\lambda_2\rangle\leftrightarrow|\lambda_4\rangle$. The $\gamma^R(\omega)=2\pi\sum_l|g_{R,l}|^2\delta(\omega-\omega_{R,l})$ denotes the spectral coupling density of the bath R at frequency ω. For simplicity, we suppose that $\gamma_i^R(\omega_n)=\gamma_i^R$ are frequency-independent throughout the paper. The collective damping rate is $\gamma_{AB}^R(\omega_n)=\sqrt{\gamma_A^R(\omega_n)\gamma_B^R(\omega_n)}=\sqrt{\gamma_A^R\gamma_B^R}=\gamma_{AB}^R$. The average photon number $\bar n^R(\omega_n)$ of the bath R depends on temperature T_R and takes Bose distribution as

$$\bar n^R(\omega_n)=\frac{1}{\exp(\omega_n/T_R)-1}. \tag{10}$$

By substituting Eqs. (8)–(10) into the equation of motion (7), we can obtain the master equation

$$\begin{aligned}\dot\rho=&-{\rm i}\left[H_{\rm S},\rho\right]+\Gamma_1L_{\tau_{43}}(\rho)+\Gamma_2L_{\tau_{21}}(\rho)+\Gamma_3L_{\tau_{34}}(\rho)\\&+\Gamma_4L_{\tau_{12}}(\rho)+\Gamma_5L_{\tau_{31}}(\rho)+\Gamma_6L_{\tau_{42}}(\rho)+\Gamma_7L_{\tau_{13}}(\rho)\\&+\Gamma_8L_{\tau_{24}}(\rho)+2(\Lambda_1\tau_{43}\rho\tau_{12}+\Lambda_2\tau_{34}\rho\tau_{21}\\&+\Lambda_3\tau_{31}\rho\tau_{24}+\Lambda_4\tau_{13}\rho\tau_{42}+{\rm h.c.}).\end{aligned} \tag{11}$$

Here, $L_X(\rho)\equiv2X\rho X^+-\{X^+X,\rho\}$ with X being an arbitrary system operator, $\tau_{\rm pq}=|\lambda_p\rangle|\lambda_q\rangle$, and

$$\begin{aligned}\Gamma_1=&\left(C_{\rm I}^A\sqrt{\gamma_A^a}-C_{\rm I}^B\sqrt{\gamma_B^a}\right)^2\left[\bar n^a(\omega_1)+1\right]\\&+\left(C_{\rm I}^A\sqrt{\gamma_A^b}-C_{\rm I}^B\sqrt{\gamma_B^b}\right)^2\left[\bar n^b(\omega_1)+1\right]=\Gamma_1'+\Gamma_1'',\\\Gamma_2=&\left(C_{\rm I}^A\sqrt{\gamma_A^a}+C_{\rm I}^B\sqrt{\gamma_B^a}\right)^2\left[\bar n^a(\omega_1)+1\right]\\&+\left(C_{\rm I}^A\sqrt{\gamma_A^b}+C_{\rm I}^B\sqrt{\gamma_B^b}\right)^2\left[\bar n^b(\omega_1)+1\right]=\Gamma_2'+\Gamma_2'',\end{aligned}$$

$$
\begin{aligned}
\Gamma_3 &= \left(C_{\mathrm{I}}^{A}\sqrt{\gamma_A^a}-C_{\mathrm{I}}^{B}\sqrt{\gamma_B^a}\right)^2\bar{n}^a(\omega_1)\\
&\quad+\left(C_{\mathrm{I}}^{A}\sqrt{\gamma_A^b}-C_{\mathrm{I}}^{B}\sqrt{\gamma_B^b}\right)^2\bar{n}^b(\omega_1)=\Gamma_3'+\Gamma_3'',\\
\Gamma_4 &= \left(C_{\mathrm{I}}^{A}\sqrt{\gamma_A^a}+C_{\mathrm{I}}^{B}\sqrt{\gamma_B^a}\right)^2\bar{n}^a(\omega_1)\\
&\quad+\left(C_{\mathrm{I}}^{A}\sqrt{\gamma_A^b}+C_{\mathrm{I}}^{B}\sqrt{\gamma_B^b}\right)^2\bar{n}^b(\omega_1)=\Gamma_4'+\Gamma_4'',\\
\Gamma_5 &= \left(C_{\mathrm{II}}^{A}\sqrt{\gamma_A^a}-C_{\mathrm{II}}^{B}\sqrt{\gamma_B^a}\right)^2[\bar{n}^a(\omega_2)+1]\\
&\quad+\left(C_{\mathrm{II}}^{A}\sqrt{\gamma_A^b}-C_{\mathrm{II}}^{B}\sqrt{\gamma_B^b}\right)^2\left[\bar{n}^b(\omega_2)+1\right]=\Gamma_5'+\Gamma_5'',\\
\Gamma_6 &= \left(C_{\mathrm{II}}^{A}\sqrt{\gamma_A^a}+C_{\mathrm{II}}^{B}\sqrt{\gamma_B^a}\right)^2[\bar{n}^a(\omega_2)+1]\\
&\quad+\left(C_{\mathrm{II}}^{A}\sqrt{\gamma_A^b}+C_{\mathrm{II}}^{B}\sqrt{\gamma_B^b}\right)^2\left[\bar{n}^b(\omega_2)+1\right]=\Gamma_6'+\Gamma_6'',\\
\Gamma_7 &= \left(C_{\mathrm{II}}^{A}\sqrt{\gamma_A^a}-C_{\mathrm{II}}^{B}\sqrt{\gamma_B^a}\right)^2\bar{n}^a(\omega_2)+(C_{\mathrm{II}}^{A}\sqrt{\gamma_A^b}\\
&\quad-C_{\mathrm{II}}^{B}\sqrt{\gamma_B^b})^2\bar{n}^b(\omega_2)=\Gamma_7'+\Gamma_7'',\\
\Gamma_8 &= \left(C_{\mathrm{II}}^{A}\sqrt{\gamma_A^a}+C_{\mathrm{II}}^{B}\sqrt{\gamma_B^a}\right)^2\bar{n}^a(\omega_2)+(C_{\mathrm{II}}^{A}\sqrt{\gamma_A^b}\\
&\quad+C_{\mathrm{II}}^{B}\sqrt{\gamma_B^b})^2\bar{n}^b(\omega_2)=\Gamma_8'+\Gamma_8'',\\
\Lambda_1 &= \left[-\left(C_{\mathrm{I}}^{A}\right)^2\gamma_A^a+\left(C_{\mathrm{I}}^{B}\right)^2\gamma_B^a\right][\bar{n}^a(\omega_1)+1]\\
&\quad+\left[-\left(C_{\mathrm{I}}^{A}\right)^2\gamma_A^b+\left(C_{\mathrm{I}}^{B}\right)^2\gamma_B^b\right]\left[\bar{n}^b(\omega_1)+1\right]=\Lambda_1'+\Lambda_1'',\\
\Lambda_2 &= \left[-\left(C_{\mathrm{I}}^{A}\right)^2\gamma_A^a+\left(C_{\mathrm{I}}^{B}\right)^2\gamma_B^a\right]\bar{n}^a(\omega_1)\\
&\quad+\left[-\left(C_{\mathrm{I}}^{A}\right)^2\gamma_A^b+\left(C_{\mathrm{I}}^{B}\right)^2\gamma_B^b\right]\bar{n}^b(\omega_1)=\Lambda_2'+\Lambda_2'',\\
\Lambda_3 &= \left[\left(C_{\mathrm{II}}^{A}\right)^2\gamma_A^a-\left(C_{\mathrm{II}}^{B}\right)^2\gamma_B^a\right][\bar{n}^a(\omega_2)+1]\\
&\quad+\left[\left(C_{\mathrm{II}}^{A}\right)^2\gamma_A^b-\left(C_{\mathrm{II}}^{B}\right)^2\gamma_B^b\right]\left[\bar{n}^b(\omega_2)+1\right]=\Lambda_3'+\Lambda_3'',\\
\Lambda_4 &= \left[\left(C_{\mathrm{II}}^{A}\right)^2\gamma_A^a-\left(C_{\mathrm{II}}^{B}\right)^2\gamma_B^a\right]\bar{n}^a(\omega_2)\\
&\quad+\left[\left(C_{\mathrm{II}}^{A}\right)^2\gamma_A^b-\left(C_{\mathrm{II}}^{B}\right)^2\gamma_B^b\right]\bar{n}^b(\omega_2)=\Lambda_4'+\Lambda_4''. \qquad (12)
\end{aligned}
$$

with $C_{\mathrm{I}}^{A}=\alpha_-\beta_++\alpha_+\beta_-$, $C_{\mathrm{I}}^{B}=\alpha_-\beta_-+\alpha_+\beta_+$, $C_{\mathrm{II}}^{A}=-\alpha_-\beta_-+\alpha_+\beta_+$, and $C_{\mathrm{II}}^{B}=-\alpha_-\beta_++\alpha_+\beta_-$.

To study the stationary regime of the model, we need to solve the steady-state solution ρ^{SS} of master equation (11). By making $\dot{\rho}^{\mathrm{SS}}=0$ in Eq. (11), we obtain all off-diagonal elements $\rho_{ll'}^{\mathrm{SS}}=\langle\lambda_l|\rho^{\mathrm{SS}}|\lambda_{l'}\rangle$ with $l\neq l'$ to be zero, while the diagonal elements can be obtained as follows:

$$
\begin{aligned}
\rho_{11}^{\mathrm{SS}}&=(\Gamma_3\Gamma_4\Gamma_7+\Gamma_3\Gamma_6\Gamma_7+\Gamma_1\Gamma_4\Gamma_8+\Gamma_4\Gamma_7\Gamma_8)/A,\\
\rho_{22}^{\mathrm{SS}}&=(\Gamma_2\Gamma_3\Gamma_7+\Gamma_1\Gamma_2\Gamma_8+\Gamma_1\Gamma_5\Gamma_8+\Gamma_2\Gamma_7\Gamma_8)/A,\\
\rho_{33}^{\mathrm{SS}}&=(\Gamma_3\Gamma_4\Gamma_5+\Gamma_2\Gamma_3\Gamma_6+\Gamma_3\Gamma_5\Gamma_6+\Gamma_4\Gamma_5\Gamma_8)/A,\\
\rho_{44}^{\mathrm{SS}}&=(\Gamma_1\Gamma_4\Gamma_5+\Gamma_1\Gamma_2\Gamma_6+\Gamma_1\Gamma_5\Gamma_6+\Gamma_2\Gamma_6\Gamma_7)/A, \qquad (13)
\end{aligned}
$$

where $\rho_{ij}^{\mathrm{ss}}=\langle\lambda_i|\rho^{\mathrm{SS}}|\lambda_j\rangle$ and

$$
\begin{aligned}
A &= \Gamma_1\Gamma_4\Gamma_5+\Gamma_3\Gamma_4\Gamma_5+\Gamma_1\Gamma_2\Gamma_6+\Gamma_2\Gamma_3\Gamma_6\\
&\quad+\Gamma_1\Gamma_5\Gamma_6+\Gamma_3\Gamma_5\Gamma_6+\Gamma_2\Gamma_3\Gamma_7+\Gamma_3\Gamma_4\Gamma_7\\
&\quad+\Gamma_2\Gamma_6\Gamma_7+\Gamma_3\Gamma_6\Gamma_7+\Gamma_1\Gamma_2\Gamma_8+\Gamma_1\Gamma_4\Gamma_8\\
&\quad+\Gamma_1\Gamma_5\Gamma_8+\Gamma_4\Gamma_5\Gamma_8+\Gamma_2\Gamma_7\Gamma_8+\Gamma_4\Gamma_7\Gamma_8.
\end{aligned}
$$

3. Steady-state entanglement of IHB case and CHB case

In this work, we are interested in the steady-state entanglement between two qubits after the total system has reached a stationary state. As a figure of merit, we use the concurrence[33] to quantify the steady-state entanglement in the following sections.

Since the concurrence is defined in the bare-state representation, the evolution of the system is expressed in the eigenstate representation. Therefore, we need to obtain the transformation between the two representations as follows:

$$
\begin{aligned}
&\mu_{11}^{\mathrm{SS}}=\alpha_+^2\rho_{11}^{\mathrm{ss}}+\alpha_-^2\rho_{44}^{\mathrm{ss}},\quad \mu_{44}^{\mathrm{SS}}=\alpha_-^2\rho_{11}^{\mathrm{ss}}+\alpha_+^2\rho_{44}^{\mathrm{ss}},\\
&\mu_{22}^{\mathrm{SS}}=\beta_+^2\rho_{22}^{\mathrm{ss}}+\beta_-^2\rho_{33}^{\mathrm{ss}},\quad \mu_{33}^{\mathrm{SS}}=\beta_-^2\rho_{22}^{\mathrm{ss}}+\beta_+^2\rho_{33}^{\mathrm{ss}},\\
&\mu_{23}^{\mathrm{SS}}=\mu_{32}^{\mathrm{SS}}=\beta_+\beta_-\left(\rho_{22}^{\mathrm{ss}}-\rho_{33}^{\mathrm{ss}}\right),\\
&\mu_{14}^{\mathrm{SS}}=\mu_{41}^{\mathrm{SS}}=\alpha_+\alpha_-\left(\rho_{11}^{\mathrm{ss}}-\rho_{44}^{\mathrm{ss}}\right), \qquad (14)
\end{aligned}
$$

where $\mu_{ij}^{\mathrm{ss}}=\langle\eta_i|\rho^{\mathrm{SS}}|\eta_j\rangle$. Hence, for the so-called X-class state, the density matrix (expressed in the bare-state representation $\{|11\rangle,|10\rangle,|01\rangle,|00\rangle\}$) is given as[34]

$$
\mu^{\mathrm{SS}}=\begin{pmatrix}
\mu_{11}^{\mathrm{SS}} & 0 & 0 & \mu_{14}^{\mathrm{SS}}\\
0 & \mu_{22}^{\mathrm{SS}} & \mu_{23}^{\mathrm{SS}} & 0\\
0 & \mu_{32}^{\mathrm{SS}} & \mu_{33}^{\mathrm{SS}} & 0\\
\mu_{41}^{\mathrm{SS}} & 0 & 0 & \mu_{44}^{\mathrm{SS}}
\end{pmatrix}. \qquad (15)
$$

The concurrence is

$$
\begin{aligned}
C &= 2\max\left\{0,\left|\mu_{14}^{\mathrm{SS}}\right|-\sqrt{\mu_{22}^{\mathrm{ss}}\mu_{23}^{33}},\left|\mu_{23}^{\mathrm{SS}}\right|-\sqrt{\mu_{11}^{\mathrm{ss}}\mu_{44}^{33}}\right\}\\
&= 2\max\left\{\begin{array}{l}0,\left|\alpha_+\alpha_-\left(\rho_{11}^{\mathrm{ss}}-\rho_{44}^{\mathrm{ss}}\right)\right|-\sqrt{\left(\beta_+^2\rho_{22}^{\mathrm{ss}}+\beta_-^2\rho_{33}^{\mathrm{ss}}\right)\left(\beta_-^2\rho_{22}^{\mathrm{ss}}+\beta_+^2\rho_{33}^{\mathrm{ss}}\right)},\\ \left|\beta_+\beta_-\left(\rho_{22}^{\mathrm{ss}}-\rho_{33}^{\mathrm{ss}}\right)\right|-\sqrt{\left(\alpha_+^2\rho_{11}^{\mathrm{ss}}+\alpha_-^2\rho_{44}^{\mathrm{ss}}\right)\left(\alpha_-^2\rho_{11}^{\mathrm{ss}}+\alpha_+^2\rho_{44}^{\mathrm{ss}}\right)}\end{array}\right\}. \qquad (16)
\end{aligned}
$$

Obviously, $C=0$ means that the entanglement is zero and $C=1$ represents the maximal entanglement.

Next, we will analyze the steady-state entanglement of IHB case and CHB case respectively from the strong coupling regime and the weak coupling regime.

3.1. Strong coupling regime

Now we consider the strong coupling regime for the qubit–qubit interaction, or $\xi \geq \Omega$.

In the strong coupling regime, no matter how qubits interact with two baths—that is, for the IHB case and the CHB case—the steady-state entanglement of two coupled qubits in the case of $T_1 = T_2 = T$ is the same as that shown in Fig. 2. In Figs. 2(a) and 2(b), we plot the steady-state concurrence as a function of coupling strength ξ for various values of thermal bath temperature T and energy detuning $\Delta\Omega$, respectively. Figure 2(a) shows that the entanglement decreases with the increase of the thermal bath T and increases with ξ and reaches to 1 when the thermal bath temperature T is very small ($T = 0.015\gamma$); that is, the state becomes a maximally entangled state when the coupling is very strong coupling regime. For a larger T, the entanglement first increases and then decreases with the increase of coupling strength ξ. Figure 2(b) shows that the entanglement decreases with thermal bath T (energy detunings $\Delta\Omega$) increasing under a given energy detuning $\Delta\Omega$ (thermal bath T). In fact, the state of the two qubits at high temperature is near to the completely mixed state which contains no entanglement.

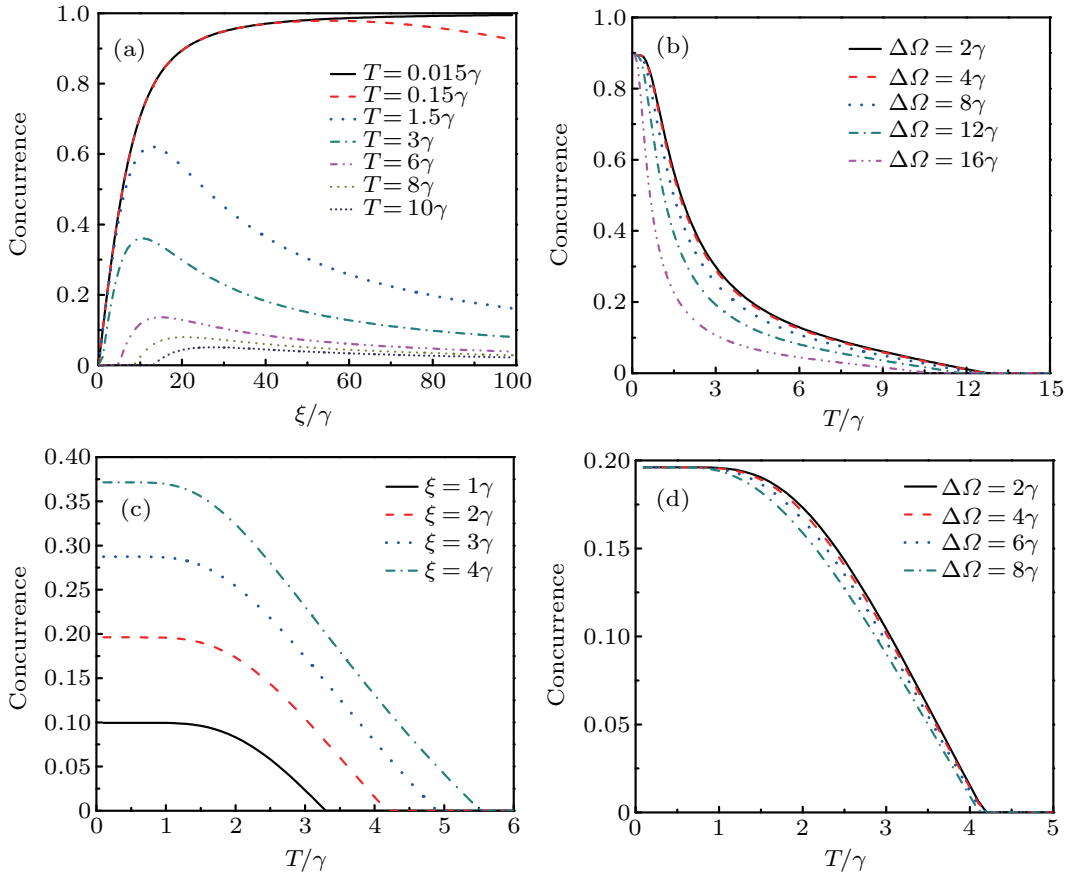


Fig. 2. In thermal equilibrium baths with $T_1 = T_2 = T$, steady-state concurrence as a function of coupling strength ξ for various temperatures of thermal baths T in panel (a). And steady-state concurrence as a function of temperature of thermal baths T for different values of coupling strength ξ in panel (c) and energy detuning $\Delta\Omega$ in panels (b) and (d). Panels (a) and (b) are for strong coupling regime; Panels (c) and (d) are for weak coupling regime. We set $\Delta\Omega = 2\gamma$ in panels (a) and (c); $\xi = 20\gamma$ in panel (b); $\xi = 2\gamma$ in panel (d). Other parameters are set to be $\gamma_A^a = \gamma_A^b = \gamma_B^a = \gamma_B^b = \gamma$ and $\Omega_m = 20\gamma$.

Next, we consider the steady-state entanglement of two coupled qubits in the nonequilibrium case with $T_1 = T_m + \Delta T/2$ and $T_2 = T_m - \Delta T/2$ where T_m denotes the average temperature and ΔT refers to the gradient of two thermal baths. For the IHB case and the CHB case, the entanglement is the same as that shown in Fig. 3(a). When the qubit–qubit interaction is not subject to RWA, we note that the concurrence decreases with the average temperature T_m increasing for $\Delta T = 0$, similar to the results in Figs. 2(a) and 2(b). In the nonequilibrium regime, we are more interested in the effect of the temperature gradient ΔT on the steady-state entanglement. As shown in Fig. 3(a), the concurrence decreases with ΔT increasing. However, compared with the entanglement with RWA in Refs. [24] and [26] at the lower average temperature T_m, the entanglement without RWA is large. So, we can obtain that the entanglement without RWA is beneficial for entanglement at lower temperature.

3.2. Weak coupling regime

Now we turn our attention to weak coupling regime for the qubit–qubit interaction, or $\xi < \Omega$.

In the weak coupling regime, the overall entanglement is small compared with in the strong coupling regime. For the IHB case and the CHB case, the steady-state entanglement of two coupled qubits in the case of $T_1 = T_2 = T$ is also the same as that shown in Fig. 2. Figure 2(c) shows that the entanglement decreases with thermal bath T increasing. For a given$T$, the entanglement increases with the coupling strength ξ increasing. Figure 2(d) shows that the entanglement decreases with thermal bath T increasing (energy detuning $\Delta\Omega$) under a given $\Delta\Omega(T)$. Likewise, when the temperature is high enough, the entanglement vanishes.

Next, we consider the steady-state entanglement of two coupled qubits in the nonequilibrium IHB case in Fig. 3(b) and CHB case in Fig. 3(c). The trend of the entanglement in Figs. 3(b) and 3(c) are the same as that shown in Fig. 3(a), but the values are different. It can be seen that the entanglement in strong coupling regime is larger than in the weak coupling regime.

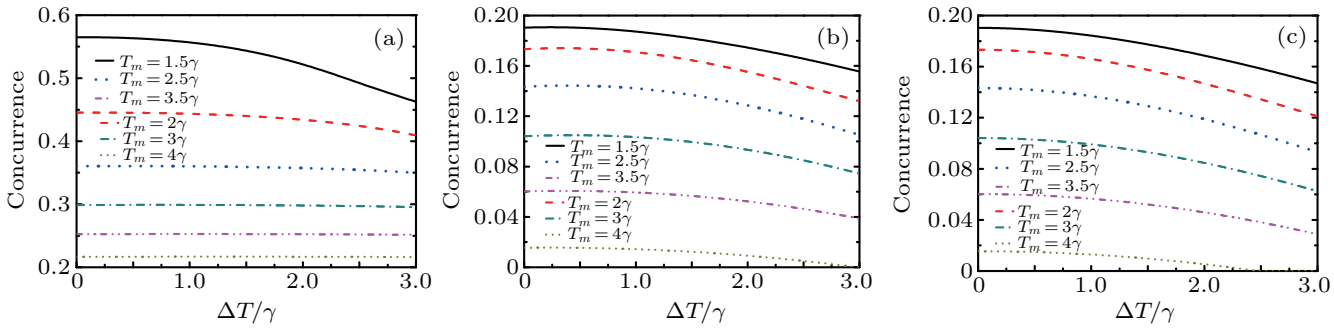


Fig. 3. In nonequilibrium thermal baths with $T_1 \neq T_2$, steady-state concurrence as a function of scaled temperature gradient of two thermal baths ΔT for different values of average temperature T_m in the strong coupling regime (a) and weak coupling regime of the IHB case (b), CHB case (c). We set $\xi = 20\gamma$ in panel (a), $\xi = 2\gamma$ in panels (b) and (c), $\Omega_m = 20\gamma$, $\Delta\Omega = 2\gamma$ and $\gamma_A^a = \gamma_A^b = \gamma_B^a = \gamma_B^b = \gamma$.

4. Heat current of IHB case and CHB case

As another figure of merit, we consider the heat current with respect to a bath R_μ defined as

$$Q_\mu = \mathrm{Tr}\left\{\zeta_\mu[\rho]H_S\right\}. \tag{17}$$

From the side of a bath, a positive heat current refers to the heat released from the bath to the system, while a negative value implies the heat absorption of the bath from the system. Therefore, a change of sign of the heat current can be used as an indicator for a crossover between heat absorption and heat release or *vice versa*.

According to Eqs. (8), (10), and (12), we can derive from Eq. (17) the explicit expressions of heat currents for the two baths as follows:

$$\begin{aligned} Q_a &= 2\left(\Gamma_4'\rho_{22}^{SS} + \Gamma_3'\rho_{44}^{SS} - \Gamma_2'\rho_{11}^{SS} - \Gamma_1'\rho_{33}^{SS}\right)\omega_1 \\ &\quad + 2\left(\Gamma_7'\rho_{33}^{SS} + \Gamma_8'\rho_{44}^{SS} - \Gamma_5'\rho_{11}^{SS} - \Gamma_6'\rho_{22}^{SS}\right)\omega_2, \end{aligned} \tag{18}$$

$$\begin{aligned} Q_b &= 2\left(\Gamma_4''\rho_{22}^{SS} + \Gamma_3''\rho_{44}^{SS} - \Gamma_2''\rho_{11}^{SS} - \Gamma_1''\rho_{33}^{SS}\right)\omega_1 \\ &\quad + 2\left(\Gamma_7''\rho_{33}^{SS} + \Gamma_8''\rho_{44}^{SS} - \Gamma_5''\rho_{11}^{SS} - \Gamma_6''\rho_{22}^{SS}\right)\omega_2. \end{aligned} \tag{19}$$

Next, we will analyze the heat current of IHB case and CHB case respectively from the strong coupling regime and the weak coupling regime.

4.1. Strong coupling regime

Figure 4(a) shows the variations of heat current Q_a and Q_b with temperature T_1 in the IHB case. For $T_1 < 20\gamma$, Q_b is positive while Q_a is negative, which implies that the heat flows from the bath b into the bath $-$ a. At the critical temperature $T_1 = 20\gamma$, the total system reaches thermal equilibrium and all heat currents become zero. When $T_1 > 20\gamma$, the heat of the bath $-$ a is transferred into bath b. Figure 4(b) shows the variations of heat current Q_a with the temperature T_1 for different values of energy detuning $\Delta\Omega$. The figures show that the larger the value of $\Delta\Omega$, the larger (smaller) the value of Q_a is when $T_1 < 20\gamma$ ($T_1 > 20\gamma$). Figure 4(c) shows that heat current Q_a decreases (increases) as coupling strength ξ increases when $T_1 > T_2 = 20\gamma (T_1 < T_2 = 20\gamma)$. For a given ξ, Q_a increases with T_1, which is consistent with the scenario in Fig. 4(a). In Fig. 4(d), the temperature at which Q_a becomes zero is the same as that in the cool bath, while a smaller lower temperature is associated with a larger the heat current.

As shown in Fig. 4(a), the variations of the heat currents Q_a and Q_b as a function of temperature T_1 have the same trend, but there is a numerical difference. Figure 5(b) shows that $\Delta\Omega$ has little effect on Q_a. Figure 5(c), indicates that Q_a decreases (increases) as the coupling strength ξ increases when $T_1 > T_2 = 20\gamma$ ($T_1 < T_2 = 20\gamma$) and Q_a is equal corresponding to the case of the coupling strength ξ large enough, (*e.g.*, for $\xi = 50\gamma$). For a given ξ, Q_a increases with T_1 increasing, which is consistent with the scenario in Fig. 5(a). In Fig. 5(d), the temperature at which Q_a becomes zero is the same as that in the cool bath, while a smaller lower temperature is associated with a larger heat current.

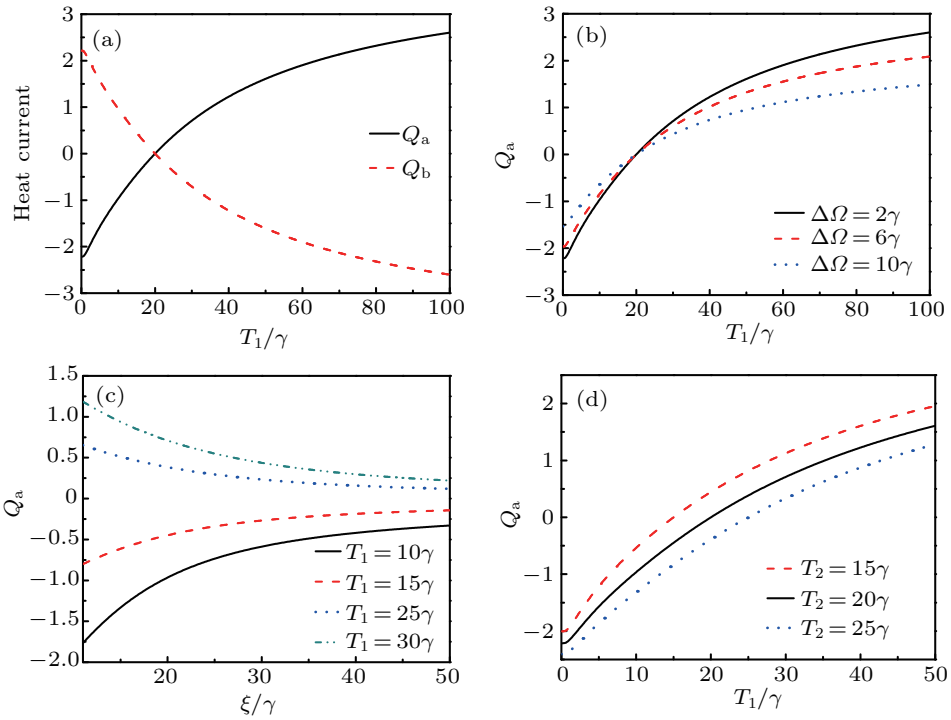


Fig. 4. In IHB case, heat currents Q_a and Q_b as a function of temperature T_1 in panel (a) and Q_a as a function of T_1 for different values of energy detuning $\Delta\Omega$ in panel (b), various values of coupling strength ξ in panel (c) and diverse values of temperature T_2 in panel (d). We set $\Delta\Omega = 2\gamma$ in panels (a), (c), and (d), $\xi = 20\gamma$ in panels (a), (b), and (d) and $T_2 = 20\gamma$ in panels (a), (b), and (c). Other parameters are set to be $\gamma_A^a = \gamma_A^b = \gamma_B^a = \gamma_B^b = \gamma$ and $\Omega_m = 20\gamma$.

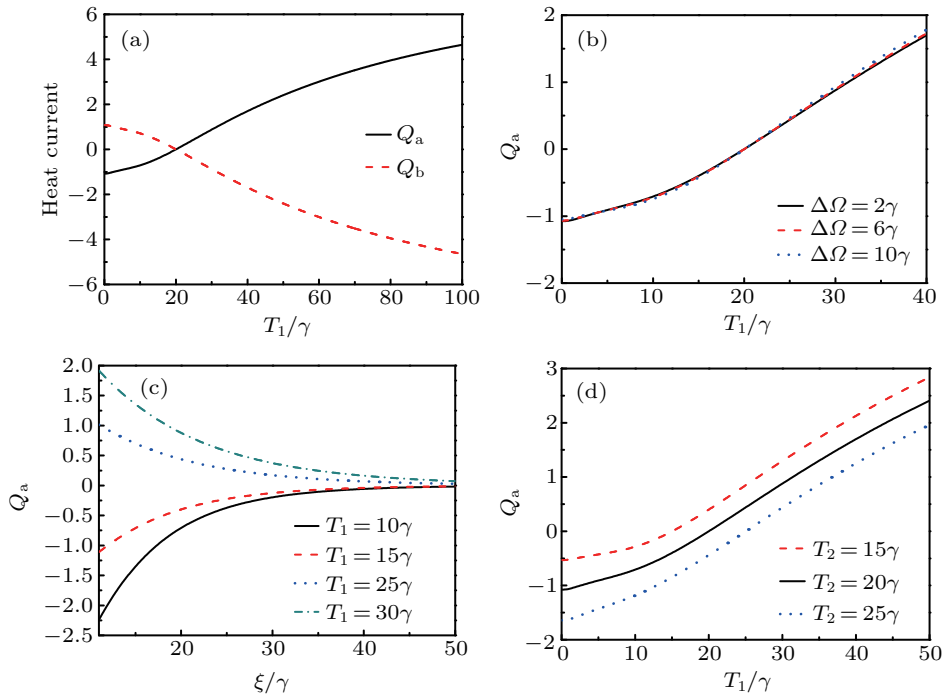


Fig. 5. In CHB case, heat currents Q_a and Q_b as a function of temperature T_1 in panel (a) and Q_a as a function of T_1 for different values of energy detuning $\Delta\Omega$ in panel (b), various values of coupling strength ξ in panel (c) and diverse values of temperature T_2 in panel (d). We set $\Delta\Omega = 2\gamma$ in panels (a), (c), and (d), $\xi = 20\gamma$ in panels (a), (b), and (d), and $T_2 = 20\gamma$ in panels (a), (b), and (c). Other parameters are set to be $\gamma_A^a = \gamma_A^b = \gamma_B^a = \gamma_B^b = \gamma$ and $\Omega_m = 20\gamma$.

4.2. Weak coupling regime

As shown in Figs. 4(a), 4(b), and 4(d), the variations of heat current Q_a and Q_b with temperature T_1 and the heat current Q_a with temperature T_1 for different values of energy detuning $\Delta\Omega$ and diverse values of lower temperature T_2 have the same trend in the IHB case, but there is a numerical difference among Figs. 6(a), 6(b), and 6(d). In Fig. 6(c), we observe that heat current Q_a first decreases and then increases with coupling strength ξ increasing when $T_1 < T_2 = 20\gamma$; for $T_1 > T_2 = 20\gamma$, Q_a increases with ξ. For a given ξ, Q_a increases with T_1 increasing, which is consistent with the scenario in Fig. 6(a).

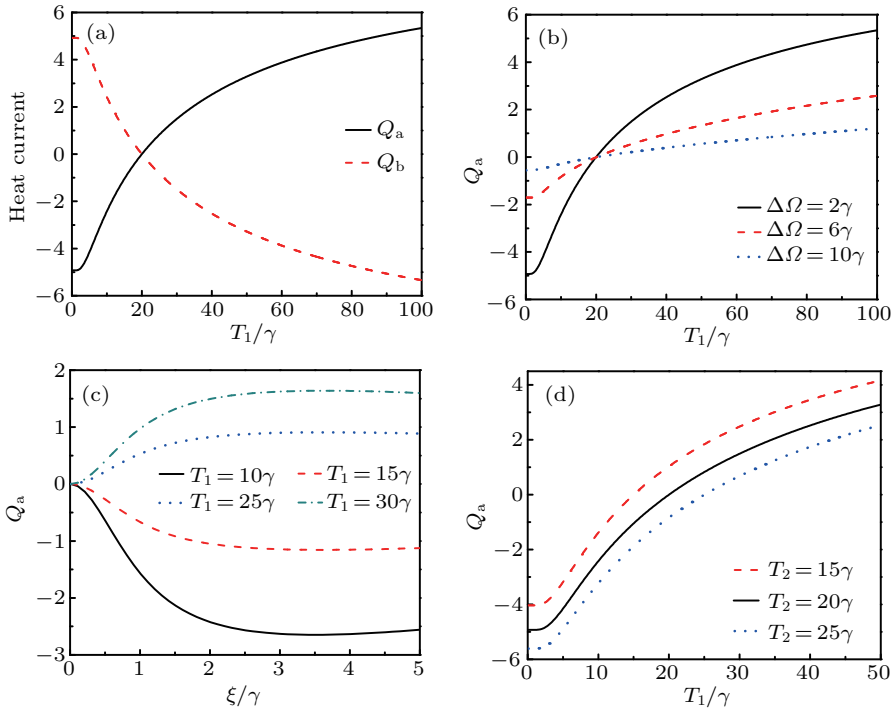


Fig. 6. In IHB case, heat currents Q_a and Q_b as a function of temperature T_1 in panel (a) and Q_a as a function of T_1 for different values of energy detuning $\Delta\Omega$ in panel (b), various values of coupling strength ξ in panel (c) and diverse values of temperature T_2 in panel (d). We set $\Delta\Omega = 2\gamma$ in panels (a), (c), and (d), $\xi = 2\gamma$ in panels (a), (b), and (d) and $T_2 = 20\gamma$ in panels (a), (b), and (c). Other parameters are set to be $\gamma_A^a = \gamma_A^b = \gamma_B^a = \gamma_B^b = \gamma$ and $\Omega_m = 20\gamma$.

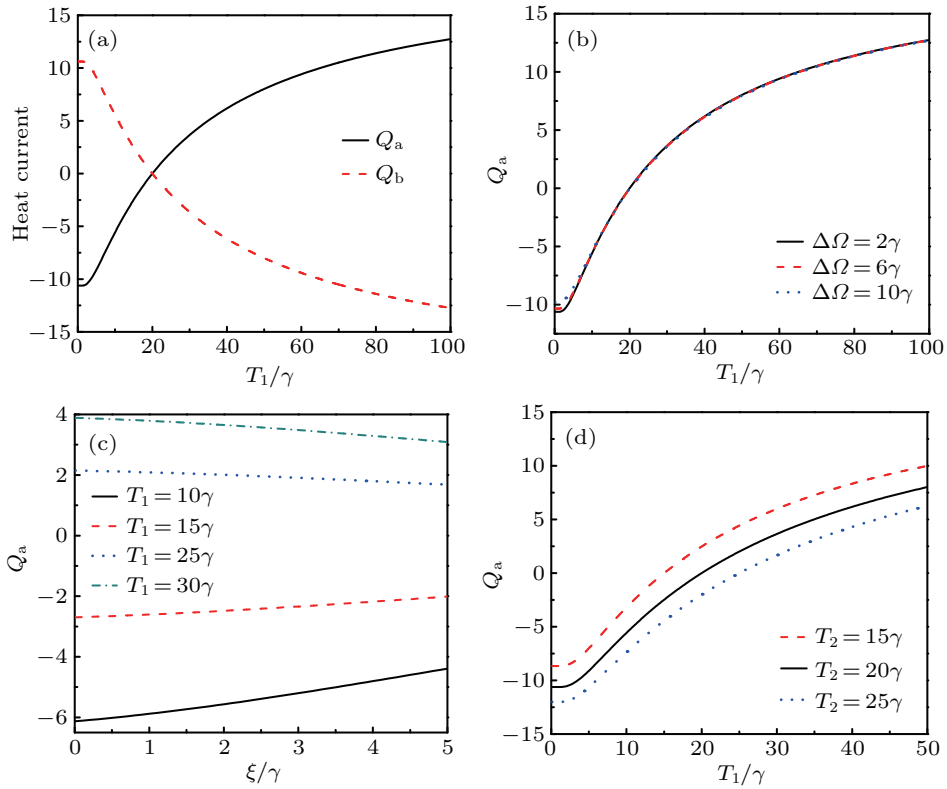


Fig. 7. In CHB case, heat currents Q_a and Q_b as a function of temperature T_1 in panel (a) and Q_a as a function of T_1 for different values of energy detuning $\Delta\Omega$ in panel (b), various values of coupling strength ξ in panel (c) and diverse values of temperature T_2 in panel (d). We set $\Delta\Omega = 2\gamma$ in panels (a), (c), and (d), $\xi = 2\gamma$ in panels (a), (b), and (d), and $T_2 = 20\gamma$ in panels (a), (b), and (c). Other parameters are set to be $\gamma_A^a = \gamma_A^b = \gamma_B^a = \gamma_B^b = \gamma$ and $\Omega_m = 20\gamma$.

As shown in Figs. 5(a), 5(b), and 5(d), the variations of heat current Q_a and Q_b with temperature T_1, the heat current Q_a with temperature T_1 for different values of energy detuning $\Delta\Omega$ and diverse values of lower temperature T_2 have the same trend in the CHB case, but there is a numerical difference among Figs. 7(a), 7(b), and 7(d). In Fig. 7(c), we observe

that heat current Q_a decreases as coupling strength ξ increase when $T_1 > T_2 = 20\gamma$; for $T_1 < T_2 = 20\gamma$, Q_a increases with ξ. For a given ξ, Q_a increases with T_1, which is consistent with Fig. 7(a).

5. Conclusions

In this work, we investigate the steady-state entanglement and heat current of two coupled qubits in two IHBs or in two CHBs. We do not make RWA for the qubit–qubit interaction, therefore we are able to investigate the behavior of the system in both the strong coupling regime and weak coupling regime.

In the strong coupling regime, for the IHB case and the CHB case, in thermal equilibrium baths, the entanglement decreases with temperature of thermal baths T increasing, and increases with coupling strength ξ increasing, and reaches to 1 when T is very small; for the larger T, the entanglement first increases and then decreases with the increase of coupling strength ξ. The entanglement decreases as T increases (energy detuning $\Delta\Omega$) under a given energy detuning $\Delta\Omega$ (thermal bath T). In nonequilibrium heat baths, for the IHB case and the CHB case, the concurrences are the same. The entanglement without RWA is useful for entanglement at lower temperatures. In a weak coupling regime, the trend of the entanglement is the same as in the strong coupling regime but the value is smaller.

Subsequently, we study the heat current of two coupled qubits. For the IHB (CHB) case, both in the strong coupling regime and in the weak coupling regime, the heat current as a function of temperature T_1 and the heat current Q_a as a function of temperature T_1 for different values of energy detuning $\Delta\Omega$ and diverse values of lower temperature T_2 have the same trend. While in the weak coupling regime, for $T_1 > T_2 = 20\gamma$ ($T_1 < T_2 = 20\gamma$), the variation trend of heat current Q_a is opposite to that of coupling strength ξ for the IHB case and the CHB case.

Thus, the IHB case and the CHB case have different behaviors in the weak coupling regime and strong coupling regime. There is also a great influence in entanglement, no matter whether or not the RWA is made. We hope that the results in this work will be useful in implementing the quantum information tasks in thermal environments.

References

[1] Horodedecki R, Horodedecki P, Horodedecki M and Horodedecki K 2009 *Rev. Mod. Phys.* **81** 865
[2] Zyczkowski K, Horodedecki P, Horodedecki M and Horodedecki R 2001 *Phys. Rev. A* **65** 012101
[3] Nielsen M and Chuang I 2000 *Quantum Information and Computation* (Cambridge: Cambridge University Press) pp. 12–15
[4] Zurek W H 2003 *Rev. Mod. Phys.* **75** 715
[5] Zhang L, Yan Y, Wu C Q, Wang J S and Li B 2009 *Phys. Rev. B* **80** 172301
[6] Zhang L, Wang J S and Li B 2010 *Phys. Rev. B* **81** 100301(R)
[7] Werlang T, Marchiori M A, Cornelio M F and Valente D 2014 *Phys. Rev. E* **89** 062109
[8] Man Z X, An N B and Xia Y J 2016 *Phys. Rev. E* **94** 042135
[9] Shen H Z, Zhou Y H and Yi X X 2014 *Phys. Rev. A* **90** 023849
[10] Ordonez-Miranda J, Ezzahri Y and Joulain K 2017 *Phys. Rev. E* **95** 022128
[11] Li B, Wang L and Casati G 2004 *Phys. Rev. Lett.* **93** 184301
[12] Joulain K, Drevillon J, Ezzahri Y and Ordonez-Miranda J 2016 *Phys. Rev. Lett.* **116** 200601
[13] Linden N, Popescu S and Skrzypczyk P 2010 *Phys. Rev. Lett.* **105** 130401
[14] Brunner N, Linden N, Popescu S and Skrzypczyk P 2012 *Phys. Rev. E* **85** 051117
[15] Mitchison M T, Woods M P, Prior J and Huber M 2015 *New J. Phys.* **17** 115013
[16] Yu C S and Zhu Q Y 2014 *Phys. Rev. E* **90** 052142
[17] Man Z X and Xia Y J 2017 *Phys. Rev. E* **96** 012122
[18] Brask J B and Brunner N 2015 *Phys. Rev. E* **92** 062101
[19] Zagoskin A M, Savel'ev S, Nori F and Kusmartsev F V 2012 *Phys. Rev. B* **86** 014501
[20] Long R and Liu W 2015 *Phys. Rev. E* **91** 062137
[21] Zhao L M and Zhang G F 2017 *Quantum Inf. Process.* **16** 216
[22] Louisell W H and Walker L R 1965 *Phys. Rev.* **137** B204
[23] Wall D F and Milburn G J 1985 *Phys. Rev. A* **31** 2403
[24] Liao J Q, Huang J F and Kuang L M 2011 *Phys. Rev. A* **83** 052110
[25] Huangfu Y and Jing J 2018 *Sci. China-Phys. Mech. Astron.* **61** 010311
[26] Hu L Z, Man Z X and Xia Y J 2018 *Quantum Inf. Process.* **17** 45
[27] Wang C and Chen Q H 2013 *New J. Phys.* **15** 103020
[28] Man Z X, Xia Y J and An N B 2011 *J. Phys. B: At. Mol. Opt. Phys.* **44** 9
[29] Deng W and Deng Y 2018 *Phys. A* **512** 693
[30] Yang Y, Wang A M, Cao L Z, Zhao J and Lu H X 2018 *Chin. Phys. B* **27** 090302
[31] Gao D Y, Gao Q and Xia Y J 2018 *Chin. Phys. B* **27** 060304
[32] Decordi G L and Vidiella-Barranco A 2017 *Opt. Commun.* **387** 366
[33] Wootters W K 1998 *Phys. Rev. Lett.* **80** 2245
[34] Yu T, Eberly J H 2007 *Quantum Inf. Comput.* **7** 459